Tailoring holes for improving the efficiency of single-mode photonic crystal waveguide lasers on InP substrate

X. Checoury,[a] P. Boucaud, X. Li, and J.-M. Lourtioz
Institut d'Électronique Fondamentale, UMR 8622 du CNRS, Université Paris-Sud, Bât. 220, 91405 Orsay Cedex, France

E. Derouin, O. Drisse, F. Poingt, L. Legouezigou, O. Legouezigou, P. Pommereau, and G.-H. Duan
Alcatel Thales III-V Lab, Alcatel Research and Innovation, Route de Nozay, 91460 Marcoussis Cedex, France

(Received 1 March 2006; accepted 21 June 2006; published online 16 August 2006)

The authors show that the use of triangular lattice photonic crystals (PhCs) with wide holes can significantly improve the lasing performances of PhC waveguides in the InP substrate approach. The study is carried out on $W_{2\text{-}3}$ waveguides made in PhCs whose air filling factor is varied from ~25% to 55%. Intrinsically single-mode laser emissions with reduced threshold (/2) are obtained when the laser mode folds deeply into the gap. Concurrently, the slope of the light-light characteristic is increased by a factor of 14. The laser spectral behavior and threshold evolution are explained from three-dimensional finite difference time domain calculations. © *2006 American Institute of Physics*.
[DOI: 10.1063/1.2335484]

Very significant progress has been accomplished during the last three years in the development of photonic crystal (PhC) microlasers.[1–9] Of particular interest for telecommunication applications is the development of single-mode PhC waveguide lasers on InP substrate with the perspective of ultracompact PhC-based circuits. As is known, the major difficulty in the substrate approach stems from the relatively low vertical confinement of light with the result that most of the waveguide modes of interest are above the light line and suffer out-of-plane diffraction losses. Perturbative analyses and three-dimensional finite difference time domain (FDTD) calculations have previously shown that the diffraction losses at the PhC holes could be strongly reduced for a sufficient hole depth while an $f \approx 30\%$ air filling factor was considered as a good compromise regarding the photonic gap width.[10,11] Indeed, recent improvements in the laser performances mostly rely on the use of an optimized deep etch process to minimize the waveguide losses.[12] However, for an air filling factor of ~30%, the dispersion curve of the fundamental waveguide mode typically folds out of the two-dimensional photonic gap, whereas operating the laser near the folding points can be strategic for obtaining a single-mode distributed feedback (DFB)-like emission with large side-mode suppression ratio.[9] One solution to overcome this difficulty is to design PhC waveguides with a multiple periodicity in such a way that the fundamental mode dispersion curve folds in the gap.[6] Another solution is to deliberately use PhC holes of large radius and thus large air filling factors and wide photonic gaps so as to allow the fundamental mode of standard PhC waveguides to fold inside the gap. Encouraging results in this second direction were recently reported in an experimental work on $W_{3\text{-}4}$ (i.e., width determined by alternating 3 and 4 missing holes) waveguide lasers, which showed that an in-gap operation reinforced the modal discrimination between the two DFB-like components of the laser emission.[8]

[a]Author to whom correspondence should be addressed; electronic mail: xavier.checoury@ief.u-psud.fr

The band diagram of PhC waveguide lasers in the InP substrate approach is schematized in Fig. 1(a) for the two main directions of the triangular lattice. The lattice period a is usually chosen to be larger than ~350 nm in order to ensure an accurate fabrication of the photonic crystal with the deep etch technique. For a laser emission near $\lambda = 1550$ nm, this corresponds to normalized frequencies a/λ above ~0.225. For the ΓK direction and W_i waveguides whose width is determined by i missing holes, only the second fold of the fundamental waveguide mode can be reached experimentally [Fig. 1(a), left]. In these conditions and for a standard air filling factor $f=30\%$, the DFB-like emission will occur above gap.[9] For the ΓM direction and $W_{i\text{-}(i+1)}$ waveguides whose widths are determined by alternating i and $(i+1)$ missing holes, only the third fold of the fundamental mode is found in the investigated spectral range [Fig. 1(a), right]. The third-order DFB emission will occur near the upper gap edge in the standard case $(f \approx 30\%)$.[9] Let us focus on this type of waveguide and vary the PhC hole radius r [i.e., the air filling factor, Fig. 1(b)]. As expected, the TE gap broadens with the hole radius and the lower gap edge

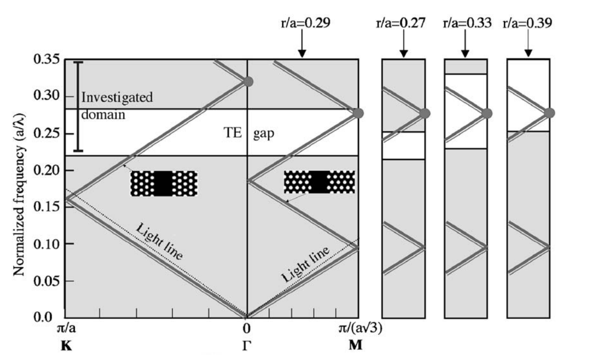

FIG. 1. (a) Schematic representation of the triangular lattice band diagram showing how the fundamental waveguide mode folds in the two lattice directions ΓK and ΓM. The ratio of the PhC hole radius to the lattice period is $r/a=0.29$ (air filling factor $f=30\%$). Insets: W_3 and $W_{2\text{-}3}$ waveguides (left and right, respectively). (b) Evolution of the band diagram near the M point with r/a (from left to right $f=26\%$, 40%, and 55%).

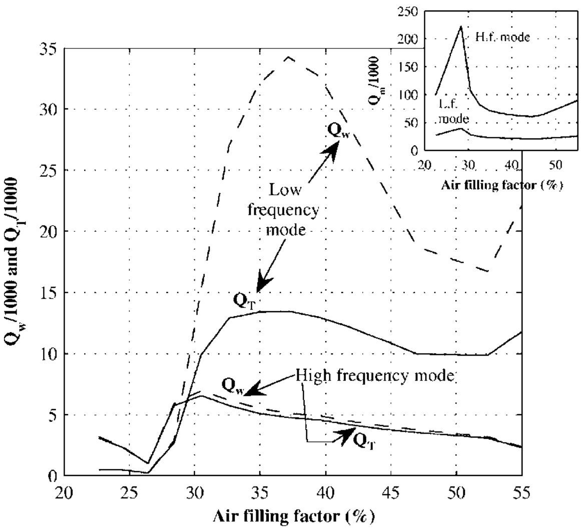

FIG. 2. Q factors of the two DFB-like components near the M point calculated vs the air filling factor f of the PhC. Dashed curves are for the infinite waveguide (Q_w) while solid curves include the influence of the end facet for the finite waveguide (Q_T). The inset shows the evolutions of the quality factor associated with the facet reflectivity (Q_m) for the two modes. Calculations are performed from a 3D FDTD model.

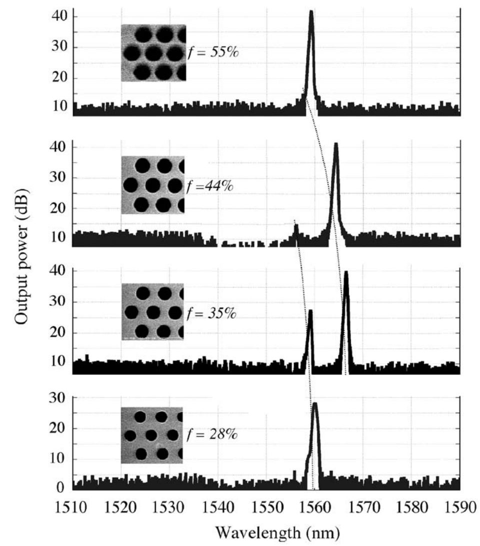

FIG. 3. Emission spectra of $W_{2\text{-}3}$ waveguide lasers measured for four values of the air filling factors. Dotted curves are used to indicate the wavelength evolutions of the low- and high-frequency DFB components. Insets show scanning electron microscope images of the corresponding PhCs near a $W_{2\text{-}3}$ waveguide edge.

rises up, but in first approximation, the folding frequency at the M point remains constant. The net result is that for increasing values of the hole radius, the third-order DFB-like emission of $W_{i\text{-}(i+1)}$ lasers can successively occur above gap, near the upper gap edge and deeply in the gap. Very low in-plane losses are expected in the latter case. However, because of the low vertical confinement of light in the substrate approach, the DFB frequencies lie above the light line in any case. In other words, out-of-plane diffraction losses can never be neglected.

A theoretical estimate of the quality factor Q_w (or equivalently the lifetime) of the waveguide mode near the M point can actually be made from three-dimensional (3D) FDTD calculations using Bloch boundary conditions.[8,13] Let us consider $W_{2\text{-}3}$ waveguides of infinite length. Because the real waveguides are comprised of a finite number N of periods along the propagation direction, FDTD calculations are made for the normalized wave vector closest to the M point with $k=0.5-1/(2N)$. The dashed curves in Fig. 2 represent the results of such calculations at $k=0.4983$ ($N=300$) for the two frequencies apart the mini-stop-band (the two DFB components). Solid curves in Fig. 2 will be discussed later as they include the influence of the end mirror facet. As seen, the Q_w factor evolutions calculated versus f for the two DFB components are very different. At small values of f (i.e., when the DFB emission occurs above gap), the calculated Q_w factors are modest, while the high-frequency mode component appears to be the dominant one. For standard air filling factors (i.e., when the DFB emission occurs near the upper gap edge), the Q_w factors are still modest, but have comparable values for the two DFB components. Above $f=30\%$ (i.e., when the DFB emission occurs well in gap), the Q_w factor of the high-frequency component starts to slowly decrease, while that of the low-frequency component strongly increases. A maximum is reached near $f=40\%$. A slow decrease of Q_w is then observed for larger air filling factors. Operating deeply into the gap ($f=40\%$) reinforces the confinement of the modes into the dielectric waveguide core, thereby reducing the diffraction losses at the PhC holes bordering this core. However, only the Q factor of the low-frequency component is strongly increased because this component is always more confined in the waveguide core than the high-frequency one.

The $W_{2\text{-}3}$ PhC waveguide lasers were fabricated in an InP/InGaAsP/InP laser structure including six compressively strained InGaAsP quantum wells whose emission was centered at 1550 nm. The triangular lattice of holes was defined by electron beam lithography. The lattice period was chosen to be ~430 nm. Five series of lasers with different PhC hole radii were fabricated to vary the air filling factor in the range of 25%–55%, as in the simulations. However, because of a residual conicity of the air holes, the actual values of the air filling factor were smaller than the expected ones. The holes were etched around 3 μm deep through the entire semiconductor heterostructure. The $W_{2\text{-}3}$ waveguides were ~220 μm long (~300 PhC periods). They were terminated at one end by a cleaved facet, and at the other end by a PhC mirror with the same lattice period, but with a fixed hole radius $r=0.33a$ (i.e., $f=40\%$) to optimize the mirror reflectivity. An antireflecting coating was deposited on the cleaved facet. The $W_{2\text{-}3}$ waveguide lasers were operated under optical pumping. A 1.06 μm pulsed yttrium aluminum garnet laser was used for this purpose. The pulse duration was fixed to 15 ns, and the repetition rate was 10 kHz. The pump beam was focused with a cylindrical lens onto a ~10 μm wide, ~2 mm long light spot. The laser emission was spectrally resolved at the waveguide output using a monochromator and an InGaAs photodetector. Although optical pumping experiments can be seen as preliminary ones, a previous work on $W_{3\text{-}4}$ lasers has shown the excellent correspondence between the results obtained under optical pumping and those obtained under electrical pumping.[8] There is no doubt that the present results on $W_{2\text{-}3}$ could be reproduced under electrical pumping.

Figure 3 shows the $W_{2\text{-}3}$ laser emission spectra measured at room temperature for different values of the air filling factor. At small air filling factors, only one emission peak is observed in the measured spectrum. This is consistent with

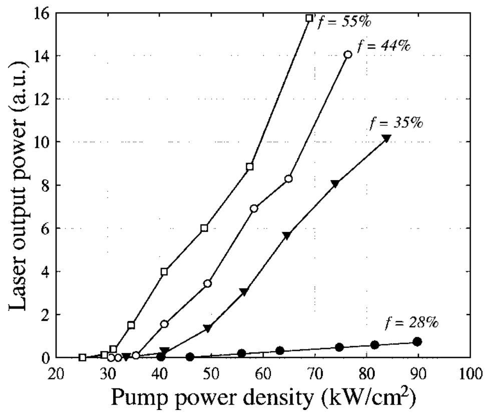

FIG. 4. Light-light characteristics of the $W_{2\text{-}3}$, laser measured for four values of the air filling factor. Dots, triangles, and squares are experimental results.

the fact that the Q_w factor of the low-frequency (long wavelength) DFB-like component is small, as predicted in Fig. 2 for small air filling factors. For standard values of the air filling factor around 30%, a double-peaked spectrum typical of a DFB laser emission is obtained: the two DFB-like components exhibit similar Q_w factors (Fig. 2). However, the separation between the two peaks ($\Delta\lambda \approx 8$ nm) is much larger than in conventional DFB lasers because of the strong interaction between the mode field and the PhC corrugations. As the major result of Fig. 3, for large air filling factors, the emission becomes single mode with a large side-mode suppression ratio. Only the low-frequency DFB component subsists in the emitted spectrum. Again, this result is in good agreement with numerical calculations of Fig. 2, which predicts the strong predominance of the low-frequency DFB component at large air filling factors. We also observe in Fig. 3 that the frequency of each mode increase slowly with the air filling factor (dotted curves). This small increase essentially reflects the decrease of the effective refractive index with the air-hole radius. This is of practical interest for an accurate lithographic tuning of the laser emission, as the measured wavelength only varies by an amount of ~5 nm for a variation of ~100 nm of the hole diameter.

Figure 4 shows the light-light (L-L) characteristics of the $W_{2\text{-}3}$ lasers measured for various air filling factors from 28% to 55%. The laser output power is obtained by numerically integrating the measured spectrum around the main emission peak(s). As seen, the laser threshold systematically decreases with increasing values of f: a reduction by a factor of ~2 is obtained over the range of experimental investigations. At the same time, the slope of the L-L characteristic above threshold is increased by a factor of ~14. For a large part, these results are in agreement with theoretical predictions of Fig. 2, which reveal a steep increase of the Q_w factor of the low-frequency DFB component as soon as the fundamental mode deeply penetrates into the gap at the M point. However, one would have expected optimum lasing conditions, i.e., a minimum laser threshold and a maximum L-L slope, for the midgap situation which is theoretically achieved near $f \approx 38\%$ (dashed curve in Fig. 2). Actually, the discrepancy between calculations for infinite waveguides and experiments on finite waveguides is mostly explained by the influence of the output facet reflectivity and the residual conicity of the etched holes. The facet reflectivity can be described in terms of another quality factor Q_m, whose estimated value at $k=0.4983$ (Refs. 14 and 15) is plotted in the inset of Fig. 2 versus the air filling factor of the PhC. The evolution of Q_m actually reflects that of the mode group velocity, which is considerably slowed down for values of f between 20% and 30%. The overall quality factor of the guided modes for finite waveguides then writes $Q_T = (Q_w^{-1} + Q_m^{-1})^{-1}$, the evolution of which is represented in Fig. 2 for each mode (solid curves). As seen, the ratio between the maximum and minimum values of Q_T for the dominant mode is around 4, not far from the threshold reduction measured in the experiments. The laser output efficiency defined as Q_T/Q_m increases by a factor of ~14 when f is increased from 23% to 40%. This is also in agreement with the evolution of the slope of the L-L characteristic, which is found in the experiments. Besides, the residual conicity of air holes measured from scanning electron microscope images is presently estimated to reduce the effective filling factor by an amount of 5%–10% as well as the maximum achieved for Q_w. This obviously puts the experimental evolutions still closer to theoretical predictions.

In conclusion, we have shown the interest of using photonic crystals with large air filling factors for PhC waveguide lasers in the InP substrate approach. Intrinsically single-mode laser emissions with lower threshold and larger side-mode suppression ratio can be obtained when the fundamental mode dispersion curve folds deeply into the gap. These DFB-like PhC waveguide lasers can not only be more compact than conventional DFB lasers, but they are also intrinsically single mode and appear to be of great promise for low noise sources in future photonic integrated circuits.

[1] A. Sugitatsu and S. Noda, Electron. Lett. **39**, 213 (2003).
[2] T. D. Happ, M. Kamp, A. Forchel, J. L. Gentner, and L. Goldstein, Appl. Phys. Lett. **82**, 4 (2003).
[3] J. Mouette, C. Seassal, X. Letartre, P. Rojo-Romeo, J. L. Leclerc, P. Regreny, P. Viktorovitch, E. Jalaguier, P. Perreau, and H. Moriceau, Electron. Lett. **39**, 526 (2003).
[4] K. Inoue, H. Sasaki, K. Ishida, Y. Sugimoto, N. Ikeda, Y. Tanaka, S. Ohkouchi, Y. Nakamura, and K. Asakawa, Opt. Express **12**, 5502 (2004).
[5] H.-G. Park, S.-H. Kim, S.-H. Kwon, Y.-G. Ju, J.-K Yang, J.-H. Baek, S.-B. Kim, and Y.-H. Lee, Science **305**, 1444 (2004).
[6] A. Talneau, L. LeGratiet, J. L. Gentner, A. Berrier, M. Mulot, S. Anand, and S. Olivier, Appl. Phys. Lett. **85**, 1913 (2004).
[7] S. Manhkopf, M. Arlt, M. Kamp, V. Colson, G.-H. Duan, and A. Forchel, IEEE Photonics Technol. Lett. **16**, 353 (2004).
[8] X. Checoury, P. Crozat, J.-M. Lourtioz, F. Pommereau, C. Cuisin, E. Derouin, O. Drisse, L. Legouezigou, O. Legouezigou, F. Lelarge, F. Poingt, G. H. Duan, S. Bonnefont, D. Mulin, J. Valentin, O. Gauthier-Lafaye, F. Lozes-Dupuy, and A. Talneau, Opt. Express, **13**, 6947 (2005).
[9] X. Checoury, P. Boucaud, J.-M. Lourtioz, F. Pommereau, C. Cuisin, E. Derouin, O. Drisse, L. Legouezigou, O. Legouezigou, F. Lelarge, F. Poingt, G. H. Duan, S. Bonnefont, D. Mulin, J. Valentin, O. Gauthier-Lafaye, F. Lozes-Dupuy, and A. Talneau, IEEE J. Sel. Top. Quantum Electron. **11**, 1180 (2005).
[10] H. Benisty, D. Labilloy, C. Weisbuch, C. J. M. Smith, T. F. Krauss, A. Béraud, D. Cassagne, and C. Jouanin, Appl. Phys. Lett. **76**, 532 (2000).
[11] M. Kafesaki, C. M. Soukoulis, and M. Agio, J. Appl. Phys. **96**, 4033 (2004).
[12] F. Pommereau, L. Legouezigou, S. Hubert, S. Sainson, J. P. Chandouineau, S. Fabre, G. H. Duan, B. Lombardet, R. Ferrini, and R. Houdre, J. Appl. Phys. **95**, 2242 (2004).
[13] Q. Chen, Y.-Z. Huang, W.-H. Guo, and Li-Juan Yu, Opt. Commun. **248**, 309 (2005).
[14] Q_m can be estimated considering the PhC cavity as a standard Fabry-Pérot resonator whose refractive index is replaced by the group index of the PhC waveguide Ref. 15. Hence $Q_m \approx -(2\pi n_g/\lambda)\cdot(2L/\ln(R_{\text{eff}}))$ where n_g is the group index, L is the length of the cavity and R_{eff} is the effective reflectivity of the facet. R_{eff} is given by $R_{\text{eff}} \approx (n_g - 3.2)/(n_g + 3.2)$, where the number 3.2 is the refractive index of the antireflecting coating).
[15] L. Florescu, K. Busch, and S. John, J. Opt. Soc. Am. B **19**, 2215 (2002).